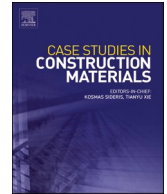




ELSEVIER

Contents lists available at ScienceDirect

## Case Studies in Construction Materials

journal homepage: [www.elsevier.com/locate/cscm](http://www.elsevier.com/locate/cscm)

# Preparation and properties of phosphogypsum-based calcined coal gangue composite cementitious materials

Haoyun Ren<sup>a</sup>, Ruiyong Mao<sup>a</sup>, Hongwei Wu<sup>b</sup>, Xing Liang<sup>c</sup>, Jiri Zhou<sup>d</sup>,  
Zujing Zhang<sup>a,\*</sup>

<sup>a</sup> College of Civil Engineering, Guizhou Provincial Key Laboratory of Rock and Soil Mechanics and Engineering Safety, Guizhou University, Guiyang 550025, China

<sup>b</sup> School of Physic, Engineering and Computer Science, University of Hertfordshire, Hatfield AL10 9AB, United Kingdom

<sup>c</sup> School of Computer Science and Mathematics, Kingston University London, KT1 2EE, United Kingdom

<sup>d</sup> China MCC5 Group CORP. LTD, China

## ARTICLE INFO

## Keywords:

Original phosphogypsum  
Calcined coal gangue  
Foam cementing material  
Orthogonal experiments  
Hydration mechanism

## ABSTRACT

Phosphogypsum (PG) and coal gangue (CG), as the largest solid waste today, the effective utilization of this part of the resource can help to alleviate environmental pollution and resource waste. The aim of this study was to utilize the excellent thermal insulation properties of original PG and the regulation of hydration products by calcined coal gangue (CCG) to produce phosphogypsum-based calcined coal gangue composite cementitious materials (PBCM). The optimal ratio of PBCM was studied through a combination of mechanical properties and thermal insulation properties. Finally, the effect of the foam factor is further investigated. The results show that: CCG can be used as a silicon-rich material with gelling properties to regulate the hydration products generated. The test block with a foam content of 8 % has the best performance, with a compressive strength of 2.53 MPa and a thermal conductivity of 0.1427 W/(m·K). The optimal experimental scheme obtained from the orthogonal test was as follows: The optimal experimental design obtained from orthogonal experiments was as follows: PG, quicklime (QL), sulfoaluminate cement (SAC) and foam contents were 45 %, 8 %, 8 % and 8 %, respectively. The CCG: cement and water-solid ratios (W/S) were 3:7 and 0.275, respectively. The development of high-performance composites presented in this study is conducive to enhancing waste utilization and provides a novel approach as well as a theoretical foundation for insulating building materials in practical engineering applications.

## 1. Introduction

Nowadays, nearly 300 million tons of phosphogypsum (PG) are produced every year in the world, of which China accounts for 1/4 of this amount, ranking first in the world [1–3]. In China, the total stockpile of PG exceeds 700 million tonnes and is steadily increasing every year [4,5]. The primary solid waste generated in the wet phosphoric acid process is known as PG [6,7]. Its chemical composition

*Abbreviation:* PG, Phosphogypsum; CG, Coal gangue; CCG, Calcined coal gangue; PBCM, Phosphogypsum-based calcined coal gangue composite cementitious materials; QL, Quicklime; WR, Water reducer; SAC, Sulfoaluminate cement; W/S, Water-solid ratios; FPBCM, Foamed phosphogypsum-based calcined coal gangue composite cementitious material; XRF, X-ray fluorescence; SEM, Scanning electron microscope.

\* Corresponding author.

E-mail address: [zjzhang3@gzu.edu.cn](mailto:zjzhang3@gzu.edu.cn) (Z. Zhang).

<https://doi.org/10.1016/j.cscm.2024.e03963>

Received 21 June 2024; Received in revised form 21 October 2024; Accepted 5 November 2024

Available online 6 November 2024

2214-5095/Crown Copyright © 2024 Published by Elsevier Ltd. This is an open access article under the CC BY license (<http://creativecommons.org/licenses/by/4.0/>).

### Nomenclature

- a The importance of compressive strength.  
b The importance of thermal conductivity.

#### Greek letters

- $\beta$  The membership degree of compressive strength.  
 $\theta$  The inverse membership degree of thermal conductivity.

**Table 1**  
Main chemical components (wt%).

Composition (%)	Al <sub>2</sub> O <sub>3</sub>	CaO	Fe <sub>2</sub> O <sub>3</sub>	K <sub>2</sub> O	MgO	Na <sub>2</sub> O	TiO <sub>2</sub>	SiO <sub>2</sub>	SO <sub>3</sub>	P <sub>2</sub> O <sub>5</sub>
PG	0.37	43.25	0.51	0.07	0.04	0.04	0.07	1.88	52.66	0.87
CCG	21.60	0.80	4.30	1.55	0.95	1.05	2.23	61.26	—	0.06
QL	0.10	99.27	0.11	—	0.20	—	—	0.15	0.13	0.01

**Table 2**  
Cement inspection report.

Cement category	Chemical evaluation index (%)				Specific surface area (m <sup>2</sup> /kg)	Solidification time (min)		Flexural strength (MPa)			Compressive strength (MPa)		
	Burning loss	SO <sub>3</sub>	MgO	Cl <sup>-</sup>		Initial setting time	Final setting time	1d	3d	7d	1d	3d	7d
P·O42.5	2.45	2.49	2.76	0.03	330	233	286	—	5.80	—	—	29.80	—
L·SAC 42.5	—	—	—	—	410	10	13	6.50	—	7.50	38.90	—	50.00

**Table 3**  
Parameters of experimental cases.

Case	PG	CCG: Cement	QL	SAC	W/S
1	40 %	3:7	2 %	4 %	0.275
2	40 %	4:6	4 %	6 %	0.300
3	40 %	5:5	6 %	8 %	0.325
4	40 %	6:4	8 %	10 %	0.350
5	45 %	3:7	4 %	8 %	0.350
6	45 %	4:6	2 %	10 %	0.325
7	45 %	5:5	8 %	4 %	0.300
8	45 %	6:4	6 %	6 %	0.275
9	50 %	3:7	6 %	10 %	0.300
10	50 %	4:6	8 %	8 %	0.275
11	50 %	5:5	2 %	6 %	0.350
12	50 %	6:4	4 %	4 %	0.325
13	55 %	3:7	8 %	6 %	0.325
14	55 %	4:6	6 %	4 %	0.350
15	55 %	5:5	4 %	10 %	0.275
16	55 %	6:4	2 %	8 %	0.300

primarily comprises CaSO<sub>4</sub>·2 H<sub>2</sub>O, along with a small amount of harmful impurities [8–10]. Furthermore, during the coal mining, refining, and washing stages, a solid waste known as (coal gangue) CG is produced, which accounts for 10~15 % of the total coal mined [11,12]. The chemical composition of CG is mainly composed of SiO<sub>2</sub> and Al<sub>2</sub>O<sub>3</sub> [13]. Currently, China's annual CG production can reach up to 15 billion tons, and the cumulative stockpile has exceeded 200 billion tons, covering an area of approximately 12,000 ha [14–17]. When large quantities of PG and CG are stored on land, harmful components in these materials will seep into the ground or sink into rivers with the surface water, polluting the soil and water quality, and endangering human health and the ecological environment [18–20]. Therefore, it is crucial to develop innovative technologies and methods to effectively utilize PG and CG, thereby minimizing environmental impact caused by solid waste.

The extensive utilization and development of PG in China has been occurring for over 40 years, with significant advancements in the technology for utilizing and developing PG resources. Gu et al. [21] utilized the use of PG as a soil stabilizer. The researchers observed that the mechanical strength of the soil stabilized with 3 % of PG was the highest, and a small amount of PG was able to form

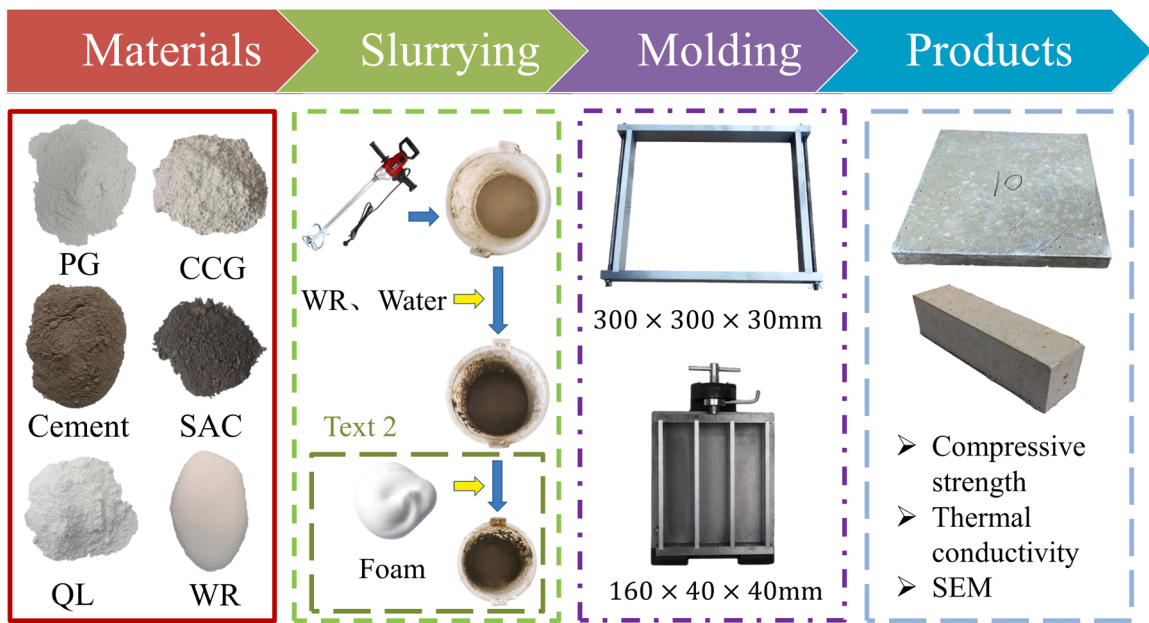


Fig. 1. Sample preparation and test diagrams.

Table 4  
Orthogonal test table.

Groups	28 d Compressive strength (MPa)	Thermal conductivity (W/(m · K))	Membership of compressive strength	Inverse membership of thermal conductivity	Composite score
1	6.26	0.1849	0.56	0.69	0.62
2	7.63	0.2222	0.78	0.33	0.55
3	8.23	0.2033	0.87	0.51	0.69
4	6.14	0.1948	0.54	0.59	0.57
5	9.03	0.1731	1.00	0.81	0.90
6	9.05	0.2154	1.00	0.39	0.70
7	5.22	0.1684	0.39	0.85	0.62
8	5.10	0.1531	0.38	1.00	0.69
9	7.59	0.2392	0.77	0.16	0.47
10	7.58	0.2088	0.77	0.46	0.61
11	2.78	0.2025	0.01	0.52	0.26
12	3.13	0.2557	0.06	0.00	0.03
13	4.94	0.1931	0.35	0.61	0.48
14	2.72	0.2278	0.00	0.27	0.14
15	6.67	0.2377	0.62	0.18	0.40
16	4.98	0.2349	0.36	0.20	0.28

calcium aluminate and C-S-H gel with cement to form an initial framework. Wang et al. [22] produced a material using hemihydrate PG as the raw material. The compressive strength of the material was proportional to the amount of hemihydrate PG within the content of 25 %. Ding et al. [23] utilized granulation technology to produce phosphogypsum-based cold-adhesive aggregates. However, excessive PG content can lead to decreases in its hydration products and compressive strength. Li et al. [24] prepared cast-in-situ PG walls, and obtained thermal insulation walls with thermal conductivity lower than 0.2 W/(m·K), indicating that PG has excellent thermal insulation performance. However, in the above studies, there is a lack of large-scale consumption of PG, which cannot meet the purpose of large-scale consumption. Some of the studies meet the consumption demand, but there are also energy losses for PG pretreatment, such as heat treatment or water washing, and secondary pollution, which increases the utilization cost of PG.

The preparation of cementitious materials from original PG is a method that can deplete PG on a large scale, but requires alkaline activators or the addition of ultrafine powders with high specific surface area and pozzolanic activity to adjust the development of strength, such as silica fume and metakaolin. Kaolin is an important component of CG, and its chemical composition is similar to that of metakaolin after heat activation at 500 ~ 800 °C [25]. At the same time, calcined gangue exhibited volcanic ash activity, which increased with the increase of kaolin content [26]. The CG (SiO<sub>2</sub> + Al<sub>2</sub>O<sub>3</sub> + Fe<sub>2</sub>O<sub>3</sub>) content with high kaolin content is more than 70 %, and the SO<sub>3</sub> content is less than 4 %, which meets the requirements of manufacturing cementitious materials (C618–23 2023) [27]. Silicon-rich materials can be reconfigured with CaO–SiO<sub>2</sub>–Al<sub>2</sub>O<sub>3</sub> ternary oxidation system to regulate the formation of hydration

**Table 5**  
Range analysis table.

Index	Level	A	B	C	D	E
28 d Compressive strength	K1	28.26	27.82	23.07	17.33	25.61
	K2	28.40	26.98	26.46	20.45	25.42
	K3	21.08	22.90	23.64	29.82	25.35
	K4	19.31	19.35	23.88	29.45	20.67
	Range	9.09	8.47	3.39	12.49	4.94
	Significant	D > A > B > E > C				
Thermal conductivity	K1	0.81	0.79	0.84	0.84	0.78
	K2	0.71	0.87	0.89	0.77	0.86
	K3	0.91	0.81	0.82	0.82	0.87
	K4	0.89	0.84	0.77	0.89	0.80
	Range	0.196	0.084	0.124	0.116	0.083
	Significant	A > C > D > B > E				
Composite score	K1	2.43	2.47	1.86	1.42	2.32
	K2	2.91	2.00	1.88	1.98	1.92
	K3	1.37	1.98	1.98	2.48	1.90
	K4	1.30	1.57	2.28	2.13	1.87
	Range	1.61	0.90	0.42	1.07	0.46
	Significant	A > D > B > E > C				

Here: A represents the content of phosphogypsum, B represents the substitution ratio of calcined coal gangue, C represents the content of quicklime, D represents the content of sulfoaluminate cement, and E represents the water solid ratio.

products to enhance mechanical properties, while CG contains a large amount of SiO<sub>2</sub> (>50 %), which can be used as silicon-rich materials to readjust the hydration products generated by reaction. Wang et al. [28] used calcined coal gangue (CCG) powder to fully replace fly ash to prepare alkali active slag materials. The results showed that the compressive strength of the test blocks increased by 4–27 % after 7 days, even though the microstructure did not significantly change. Guo et al. [29] discovered that the CG powder after heat treatment can reduce the harmful pore content and increase the harmless pore content in the hardened cement slurry. Yao et al. [30] conducted an experimental study to investigate the feasibility of using 10 %-50 % CG to replace ordinary Portland cement in the preparation of steam-cured foam concrete. The results showed that the compressive strength of CG with a 30 % substitution rate was the highest under steam curing conditions, and the dry shrinkage of foam concrete would be significantly reduced with an increase in the CG substitution rate. Guan et al. [31] utilized the microwave activation method to produce activated CG powder as a supplemental cementitious material, which demonstrated improved mechanical properties. The experimental results revealed that the CG powder produced at a microwave temperature of 600–700 °C had the best mechanical properties. Additionally, the activated CG powder can decompose the active substances in the cement hydration process, change the hydration products of cement mortar, and fill the harmful pores in the structure. Wang et al. [32] conducted a study on the effect of wet co-grinding CCG on the properties of PG-based supersulfate cementitious materials. Their experimental results indicated that the inclusion of calcination of CG can promote the formation of C-S-H gel of hydration products, thereby limiting the further crystallization of aluminite. Hence, the intensity can be adjusted by adding the appropriate amount of CCG to alter the hydration state.

In summary, PG exhibits outstanding thermal insulation properties and a relatively good compressive strength. CCG is utilized as a supplementary cementing material due to its volcanic ash activity and high SiO<sub>2</sub> content. However, there is a large accumulation of PG and CG with relatively low utilization rates, causing significant environmental pollution. In previous studies, PG were employed in smaller quantities or required pre-treatment, resulting in secondary pollution and energy consumption. In addition, there are few studies on the use of CCG to improve the utilization rate of original PG solid waste and adjust the performance of test blocks, which needs to be further explored. Therefore, FPBCM is a significant research direction, which uses PG and CCG to improve its compressive and thermal conductivity, and effectively reduce environmental pollution and energy consumption.

In order to tackle the environmental issues caused by PG and CG and maintain the sustainability of environmental development. In this paper, a new type of composite material is fabricated by adding CCG, a silicon-rich material different from cement, based on the original PG. Investigated the material's mechanical properties, thermal insulation performance, and overall performance, and analyzed the impact of foam factors on the insulation and mechanical properties of different density grades. The study revealed that the composite material exhibited exceptional thermal insulation performance while maintaining its mechanical properties. In actual engineering projects, the use of this building material helps mitigate the environmental impact associated with solid waste disposal and enhances the insulation performance of buildings, thereby reducing unnecessary energy consumption in their operation.

## 2. Materials and methods

### 2.1. Materials

The materials used in this study are PG, CCG, cement, sulfoaluminate cement (SAC), quicklime (QL), water reducer (WR), and foaming agent. Component analysis of PG, CCG, and QL is conducted using X-ray (XRF) fluorescence spectrometer, and the analysis results are shown in Table 1. PG is provided by China Guizhou Kaiphosphorus Co., Ltd., the PG used for the test is crushed with a crusher, naturally dried for 2 h, and then through the 0.15 mm square hole sieve on the sieve edge to obtain the original PG for the test,

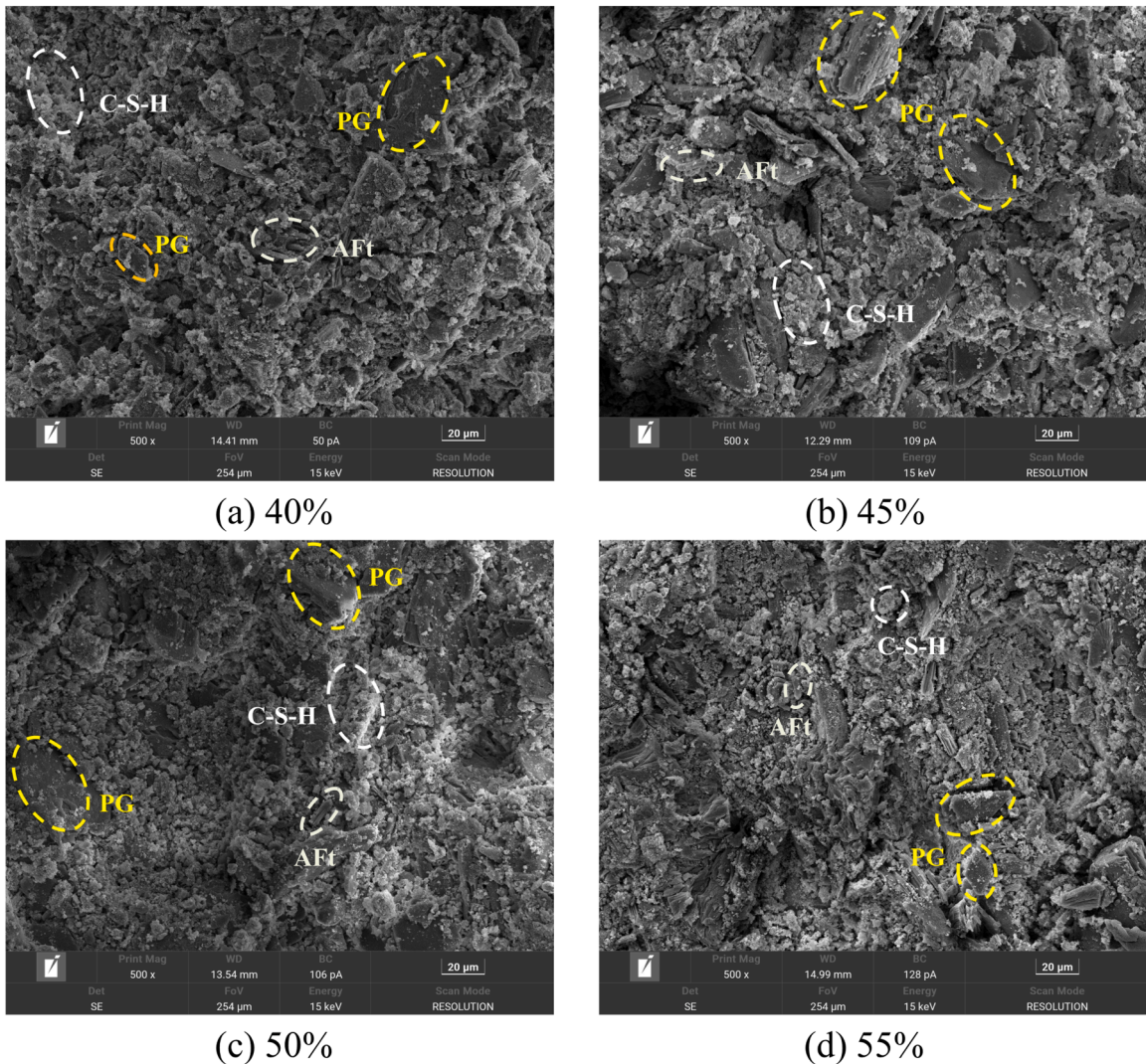


Fig. 3. SEM graphs for different PG contents.

which reduces the inhomogeneity of particle size. CG uses CCG with a calcination temperature of 700 °C and a fineness of 325 mesh provided by Hebei Lingshou Zhongtuo Building Materials Co., Ltd. QL is provided by Guiyang Xinhua Industry and Trade Co., Ltd., and the cement used in this study refers to ordinary Portland cement (P-O42.5), provided by Guiyang Conch Panjiang Cement Co., Ltd., SAC (L-SAC42.5) provided by Guiyang Zhuoyi Chemical Building Materials Co., Ltd., the inspection report is shown in Table 2. The water reducer is a polycarboxylic acid high-efficiency superplasticizer produced by Jiangsu Kaili Chemical Co., Ltd. The foaming agent is the animal protein foaming agent provided by Jinan Wenzhu Chemical Co., Ltd., which is diluted with water 1:20 and foamed by the foaming machine, which is provided by Zhejiang Tenghe Machinery Co., Ltd.

## 2.2. Protocol design

In this paper, a two-part experiment is designed for Foamed phosphogypsum-based calcined coal gangue composite cementitious material (FPBCM). In the first part, the influence of PG, cement, CCG, QL, SAC, and water-solid ratios (W/S) on the mechanical and thermal properties of phosphogypsum-based calcined coal gangue composite cementitious materials (PBCM) are studied. PG is a gas-hard cementitious material, but the gelling performance of PG in its original state is very low, so the PG content is very important for the compressive strength and thermal conductivity of PBCM. Considering the compressive strength and the amount of solid waste, the content of PG is set at 40~55%. The CCG in PBCM replaces cement with 30%, 40%, 50% and 60% of the cement content, respectively. In this study, QL is used as a base activator and SAC is used as a proagulant, and the dosages of QL and SAC are 2%, 4%, 6%, 6%, 8% and 4%, 6%, 8% and 10%, respectively. Too little water will cause the slurry to not be evenly mixed, but too much water will make the slurry unable to condense, so the water-solid ratio is set at 0.275, 0.3, 0.325, 0.35 [33,34]. Based on the above 5

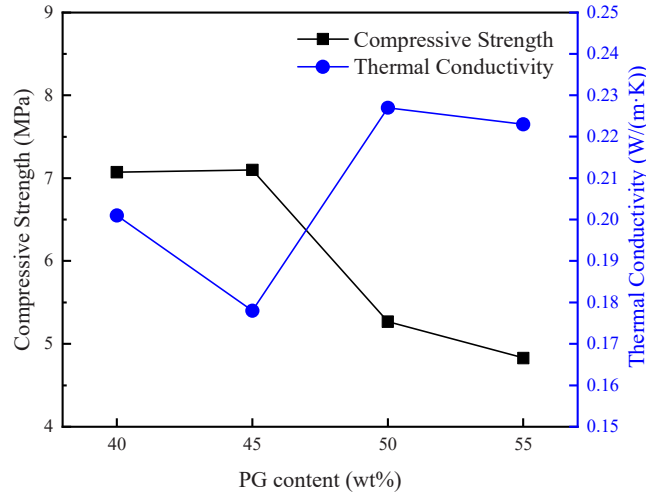


Fig. 2. Effect of PG content.

factors and 4 levels, orthogonal tests are carried out, as shown in Table 3. In the second part of the test, on the basis of the optimal scheme obtained in the first part, the influence of 0~14 % foam content on the compressive performance and thermal conductivity of FPBCM is studied.

### 2.3. Preparation of samples

As shown in Fig. 1, the raw materials are weighed according to the predetermined scheme, the dry material is stirred for 1 min, and then the required admixtures such as high-efficiency water reducer and water are added to the dry material and fully stirred for 3 min, after the slurry is stirred evenly, the foam quality required for the experimental proportion is added to the slurry, the slurry is fully stirred again, and the evenly mixed slurry is poured into the thermal conductivity test mold of 300 mm × 300 mm × 30 mm and the compressive coefficient test mold of 160 mm × 40 mm × 40 mm respectively and scrapes the surface. After the final setting of the test block, it is demolded and placed in the laboratory for natural curing to the test age.

### 2.4. Test methods

**Sample composition:** The composition of the sample is analyzed by XRF spectrometer with the model number ZSX Primus III+, Japan.

**Dry density:** put the experimental test block into the electric heating constant temperature drying oven, the temperature is 60 °C, dry to the weight constant, the weight to volume ratio is the density, the instrument model is the 101-3B electric heating constant temperature drying oven provided by Shanghai Shangpu Instrument Equipment Co., Ltd.

**Compressive properties:** After the density test, it is determined according to the method of the Chinese standard (GB/T 17669.3-1999) [35]. The equipment used is the YA-300 microcomputer controlled current servo pressure testing machine produced by Changchun Kexin Testing Instrument Co., Ltd.

**Thermal insulation performance:** measured according to the Chinese standard (GB/T 10294-2008) [36]. The equipment used in the test is the TPMBE-300 flat plate thermal conductivity meter produced by China Building Technology Group Co., Ltd., with a hot plate temperature of 35 °C and a cold plate temperature of 15 °C.

**Microstructure:** Scanning electron microscope (SEM) is used to observe the microstructure of the specimen at 28 days. Before testing, the sample needs to be sprayed with gold and vacuum treated. The instrument is the Czech TESCAN MIRA LMS.

### 2.5. Evaluation indicators

In this study, to evaluate the performance of PBCM, it is necessary to analyze the thermal conductivity and mechanical properties at the same time. The concepts of index membership and inverse index membership in the comprehensive scoring method are introduced to comprehensively evaluate the two indicators [37,38]. The formula for calculating the membership of an indicator and the membership of an inverse indicator in Eqs. 1 and 2. The Eq. 3 presents the formula for calculating the composite score.

$$\text{Index membership} = \frac{\text{Indicator value} - \text{Indicator minimum value}}{\text{Indicator maximum value} - \text{Indicator minimum value}} \quad (1)$$

$$\text{Inverse index membership} = 1 - \frac{\text{Indicator value} - \text{Indicator minimum value}}{\text{Indicator maximum value} - \text{Indicator minimum value}} \quad (2)$$

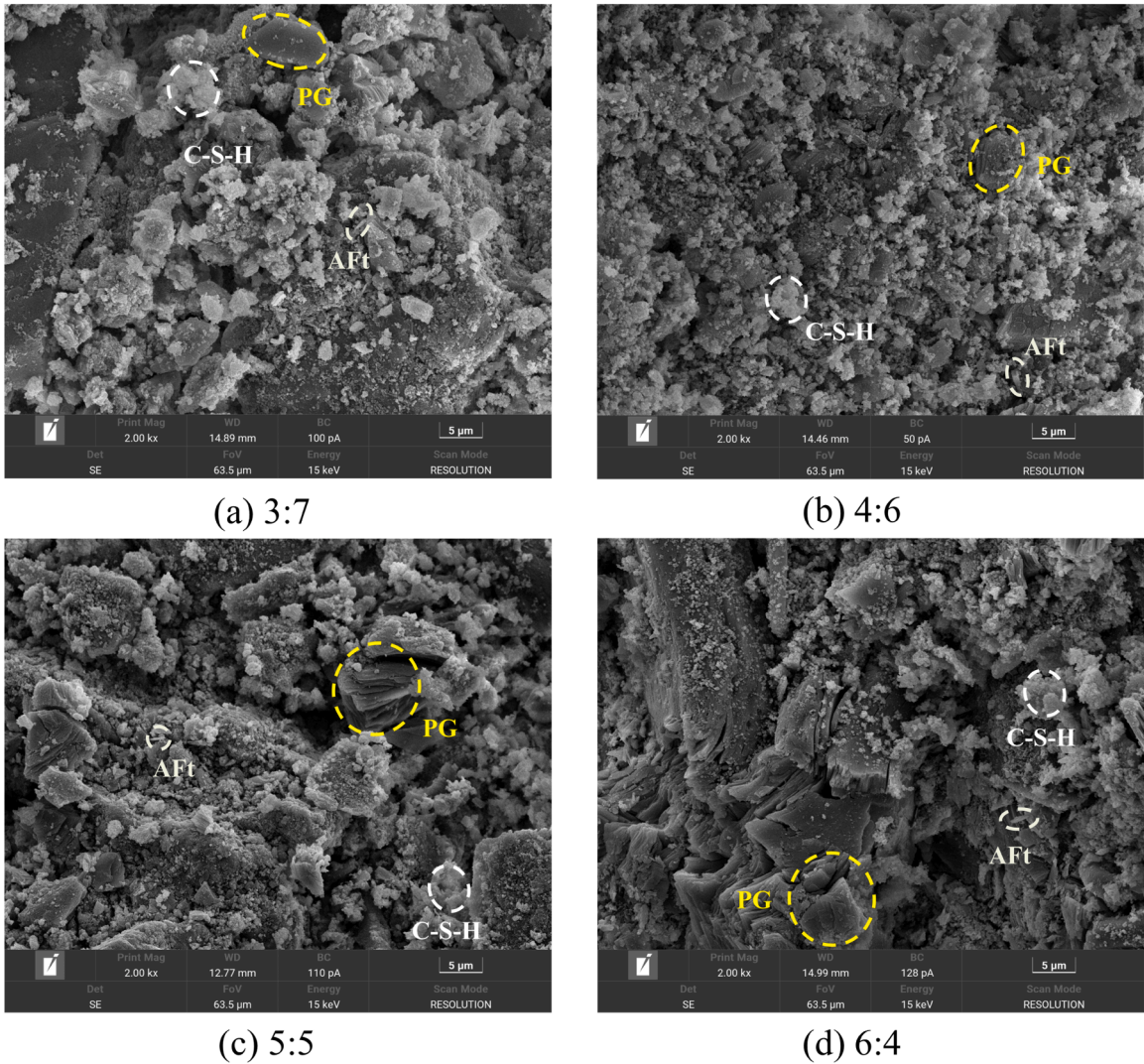


Fig. 5. SEM images with different CCG contents.

$$\text{Composite score} = a\beta + b\theta \tag{3}$$

**Note:** In this study, the importance of compressive strength and thermal conductivity is the same, so the importance of  $a$  and  $b$  is 0.5.  $\beta$  is the membership degree of compressive strength, and  $\theta$  is the inverse membership degree of thermal conductivity.

### 3. Research results

#### 3.1. Orthogonal test results

The calculated values of the compressive strength membership, thermal conductivity membership, and composite score are shown in Table 4. Table 5 is the analysis of variance for the compressive strength, thermal conductivity, and composite score. As can be seen from Table 5, the factors affecting the compressive strength of PBCM are in the following order: SAC content > PG content > CCG substitution ratio > W/S > QL content. In terms of compressive strength, the compressive strength of PBCM is the strongest when the mix ratio of PBCM is: PG content is 45 %, CCG: cement = 3:7, QL content is 4 %, SAC content is 8 %, W/S = 0.275. The factors affecting the thermal conductivity of PBCM are in the following order: PG content > QL content > SAC content > CCG substitution ratio > W/S. In terms of thermal conductivity, the thermal conductivity of PBCM is the lowest when the mixture ratio of PBCM is: PG content is 45 %, CCG: cement = 3:7, QL content is 8 %, SAC content is 6 %, W/S = 0.275. The factors affecting the compressive strength and thermal conductivity of PBCM are in the following order: SAC content > PG content > CCG substitution ratio > W/S > QL content. The comprehensive fractions of compressive strength and thermal conductivity of PBCM are analyzed, and the experimental scheme taking

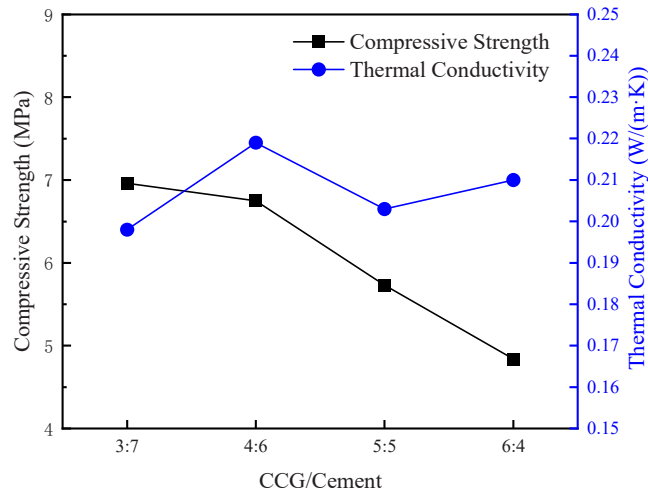


Fig. 4. Effect of CCG substitution.

into account both compressive strength and thermal conductivity is as follows: PG content is 45 %, CCG: cement = 3:7, QL content is 8 %, SAC content is 8 %, W/S = 0.275.

### 3.2. Effect of PG

Microstructure diagrams of different PG contents are shown in Fig. 3. It can be seen that with the increase of PG content, there is more PG in PBCM and less in C-S-H gel. Combined with the change trend of compressive strength and thermal conductivity in Fig. 2, with the increase of PG content from 40 % to 55 %, the compressive strength value of PBCM first increased slowly and then decreased, while the thermal conductivity value of PBCM decreased first, then increased and finally decreased steadily, and when the PG content is 45 %, the compressive strength value of PBCM is the highest and the thermal conductivity value is the lowest, which are 7.10 MPa and 0.1775 W/(m · K), respectively. The reason is that most of the mineral content in original PG is dihydrate gypsum ( $\text{CaSO}_4 \bullet 2\text{H}_2\text{O}$ ), which is directly applied to this study. Therefore, the dihydrate gypsum in the mixed slurry mostly exists in the form of filler and does not form a crystalline structure network like when dehydrated gypsum hydrates into dihydrate gypsum. Therefore, the interaction between gypsum dihydrate is mainly molecular force, and the increase of original PG content will increase the intermolecular repulsion force, thereby reducing the strength of cementitious materials.

However, the crystal structure of  $\text{CaSO}_4 \bullet 2\text{H}_2\text{O}$  in PG contains a large number of water molecules, which will form a loose structure in the crystal structure, resulting in the decrease of thermal conductivity of PBCM with the increase of PG content. When the PG content is 45 %, the molecular force between gypsum dihydrate reaches a critical point, and with the increase of PG content, the intermolecular repulsion force increases, and the connected pores and microcracks in the PEM increase, resulting in the increase of thermal conductivity and the decrease of compressive strength. Because the amount of PG content per unit volume increases, the amount of gel connected aggregate will decrease, and the loose structure in the PG crystal is prone to internal collapse and deformation when under pressure, so the thermal conductivity and compressive strength of PBCM will gradually decrease with the increase of PG content after 50 % of PG content.

### 3.3. Effect of CCG

Microstructure diagrams of different CCG dosages are shown in Fig. 5. It can be seen that with the increase of CCG content, the content of unreacted  $\text{Ca}(\text{OH})_2 \bullet 2\text{H}_2\text{O}$  gradually increases, and by Fig. 5d, the amount of unreacted PG per unit area is significantly more, and the amount of C-S-H gel is significantly less, which cannot completely cover PG. Combined with the trend of change in compressive strength and thermal conductivity in Fig. 4, with the ratio of CCG: cement from 3:7–6:4, that is, the substitution ratio of CCG decreases from 30 % to 60 %, and the compressive strength value decreases from 6.96 MPa to 4.84 MPa, which is almost linearly decreasing. The thermal conductivity value increases first and then decreases. At CCG: cement = 3:7, the compressive strength value is the highest, and the thermal conductivity value is the lowest, which are 6.96 MPa and 0.1976 W/(m · K), respectively.

The reason is that in the alkaline environment of  $\text{Ca}(\text{OH})_2$  generated by QL and Portland cement, a small amount of  $\text{Ca}(\text{SO})_4 \bullet 2\text{H}_2\text{O}$  in PG reacts with the alumina calcium in the CCG to form ettringite ( $3\text{CaO} \bullet \text{Al}_2\text{O}_3 \bullet 3\text{CaSO}_4 \bullet 32\text{H}_2\text{O}$ , Aft) as shown in Eq. 4, and the excess  $\text{Ca}(\text{OH})_2$  reacts with the  $\text{SiO}_2$  compounds in the CCG to form C-S-H gels as in Eq. 5. The addition of CCG will cause more C-S-H gels and an appropriate amount of Aft to be formed in PBCM, and the hydration products will be connected to each other and staggered between the unreacted PG, forming a denser network structure, reducing the connected pores and large cracks, and improving the compressive resistance and thermal insulation performance of PBCM. However, an excess of CCG will decrease the reaction of  $\text{Ca}(\text{OH})_2 \bullet 2\text{H}_2\text{O}$  in PG, leading to a gradual decrease in the compressive strength of PBCM and an initial increase followed by a

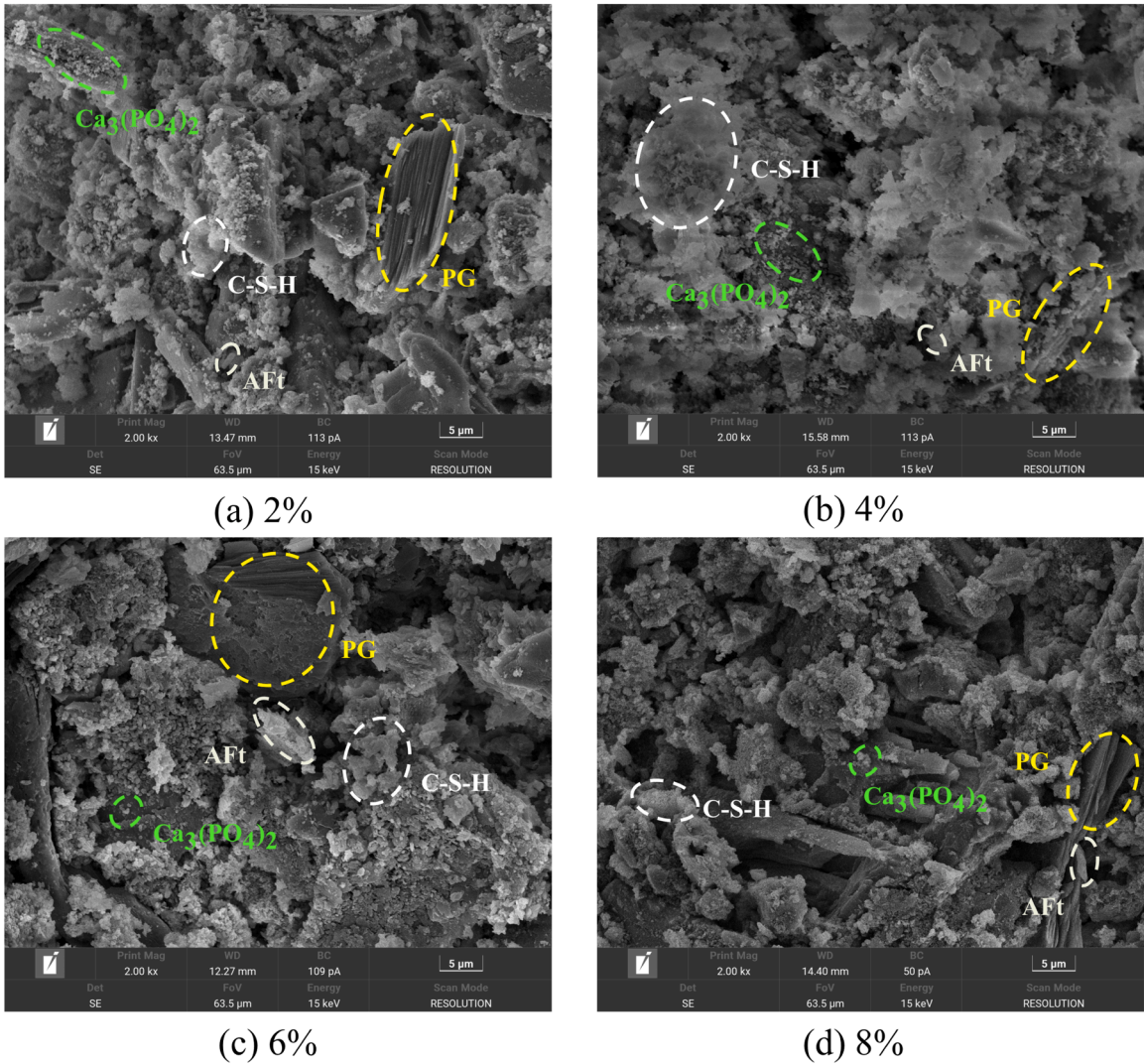
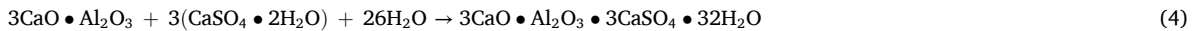


Fig. 7. SEM images with different QL contents.

decrease in the thermal conductivity value.



### 3.4. Effect of QL

Fig. 7 shows the microstructure of different QL dosages, as can be seen that the incorporated QL will neutralize the impurities in the PG and generate  $\text{Ca}_3(\text{PO}_4)_2$  to attach to the PG surface, as shown in Eq. 6. When the QL content increased from 2% to 4%, both the C-S-H gel and AFt significantly increased, while the exposed PG decreased significantly. However, when the QL content ranged from 4% to 8%, the exposed PG increased and there were gaps that were not covered by the C-S-H gel. Combined with the trend of compressive strength and thermal conductivity in Fig. 6. With the QL content from 2% to 8%, the compressive strength value of PBCM first increases, then decreases, and then increases slowly, and the thermal conductivity increases first and then decreases linearly after that. When the QL content is 4%, the compressive strength value of PBCM is 6.62 MPa, but the thermal conductivity value is also 0.2222 W/(m · K). When the QL content is 8%, the compressive strength value of PBCM is 5.97 MPa, and the thermal conductivity value is 0.1913 W/(m · K) value, which is 9.8% and 14% lower than the 4% content value, respectively. In the overall evaluation, QL content of 8% is better than a 4% performance.

The reason is that the QL hydration product is  $\text{Ca}(\text{OH})_2$ , which mainly provides the alkaline environment required for PBCM

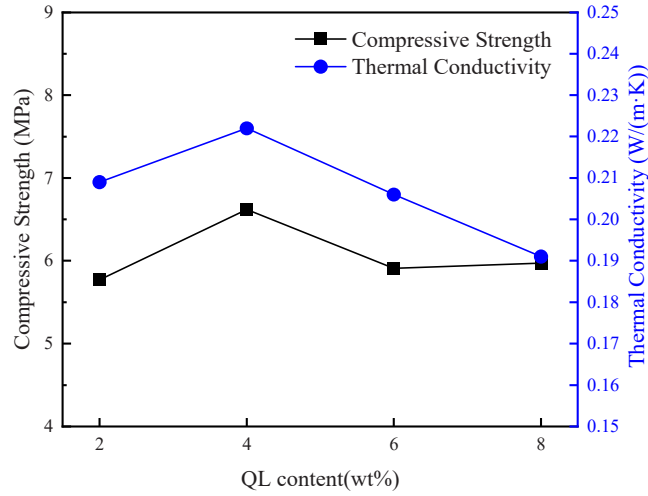


Fig. 6. Effect of QL content.

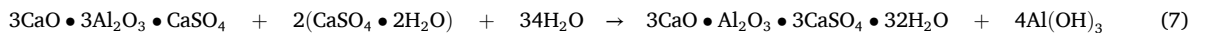
hydration, and in the mixed slurry, the  $\text{Ca}(\text{OH})_2$  will also ionize  $\text{Ca}^{2+}$  and  $\text{OH}^-$ , and the soluble phosphorus in the PG will react with the free  $\text{Ca}^{2+}$  in the slurry to form phosphoric acid compounds that are insoluble in water. When the QL content increases, there is enough  $\text{CaO}$  and  $\text{OH}^-$  to remove harmful impurities and provide the alkaline environment required for PG and CG hydration. As a result, the hydration reaction is enhanced, leading to denser PBCM with covered internal pores and cracks by hydration product connections. Consequently, both compressive strength value and thermal conductivity value are increased. However, adding an excessive amount of quicklime will lead to the oversaturation of the slurry with  $\text{Ca}(\text{OH})_2$  during the hydration process, causing it to aggregate into blocks of  $\text{Ca}(\text{OH})_2$ . A large amount of block  $\text{Ca}(\text{OH})_2$  will affect the formation of hydration products, increasing the looseness of cementitious materials. This phenomenon is manifested as a gradual decrease in the compressive strength and thermal conductivity values of PBCM.



### 3.5. Effect of SAC

Microstructure diagrams of different SAC dosages are shown in Fig. 9. It can be seen that with the increase of SAC content, the C-S-H gel increases significantly, which basically covers PG. When the SAC content is from 8% to 10%, the C-S-H gel is inhibited and significantly less. Combined with the trend of change in compressive strength and thermal conductivity in Fig. 8, with the SAC content from 4% to 10%, the compressive strength value of PBCM first increases linearly and then decreases, reaching the highest value of 7.46 MPa when the SAC content is 8%, and the thermal conductivity value decreases first and then rises linearly at 6% SAC content, and the lowest thermal conductivity value is 0.1927 W/(m·K) when the SAC content is 6%. When the SAC content is 8%, the compressive strength value of PBCM is 7.46 MPa, and the thermal conductivity value is 0.2050 W/(m·K), which is increased by 31.5% and 5.9%, respectively, compared with the SAC content of 6%. Therefore, in the overall evaluation, the performance of 8% SAC content is better.

SAC is a hydraulic cementitious material made mainly of anhydrous calcium sulfoaluminate ( $3\text{CaO} \cdot 3\text{Al}_2\text{O}_3 \cdot \text{CaSO}_4$ ) and dicalcium silicate ( $2\text{CaO} \cdot \text{SiO}_2$ ), which exhibits excellent early strength and rapid hardening properties. In high content PG gelatinous materials, PG will lead to an extremely slow hydration rate of the mixed colloid, affecting its shaping strength. However, the addition of PG in the early hydration process of SAC can play a promoting role, accelerating the hydration rate of the mixed gel material and thereby enhancing the compressive strength. The hydration mechanism is that after SAC is stirred with water, anhydrous calcium sulfoaluminate will react with gypsum dihydrate and water to form Aft and aluminum gel ( $\text{Al}(\text{OH})_3$ ,  $\text{AH}_3$ ), as shown in Eq. 7.  $\text{AH}_3$  has a higher van der Waals force than C-S-H, and can intersect with Aft in the early hydration process to fix the PG crystal and improve the compressive strength. Dicalcium silicate in SAC also reacts with water to form C-S-H gel and  $\text{Ca}(\text{OH})_2$ , thereby improving compressive strength and providing an alkaline environment, as shown in Eq. 8. In the alkaline environment,  $\text{AH}_3$  will consume a part of PG to generate Aft, which further improves the hydration rate and compressive strength of PBCM, as shown in Eq. 9. With the increase of SAC content, the content of anhydrous calcium sulfoaluminate and dicalcium silicate increased, and the Aft,  $\text{AH}_3$  and C-S-H gels generated by hydration reaction also increased, and  $\text{AH}_3$  and C-S-H will be filled and appended to the pores and cracks of the rubber material, reducing the large cracks and forming more independent pores. However, excessive SAC will fill the tiny pores of the formed  $\text{AH}_3$  and generate a large amount of Aft, thereby reducing the thermal insulation performance and compressive strength of PBCM.



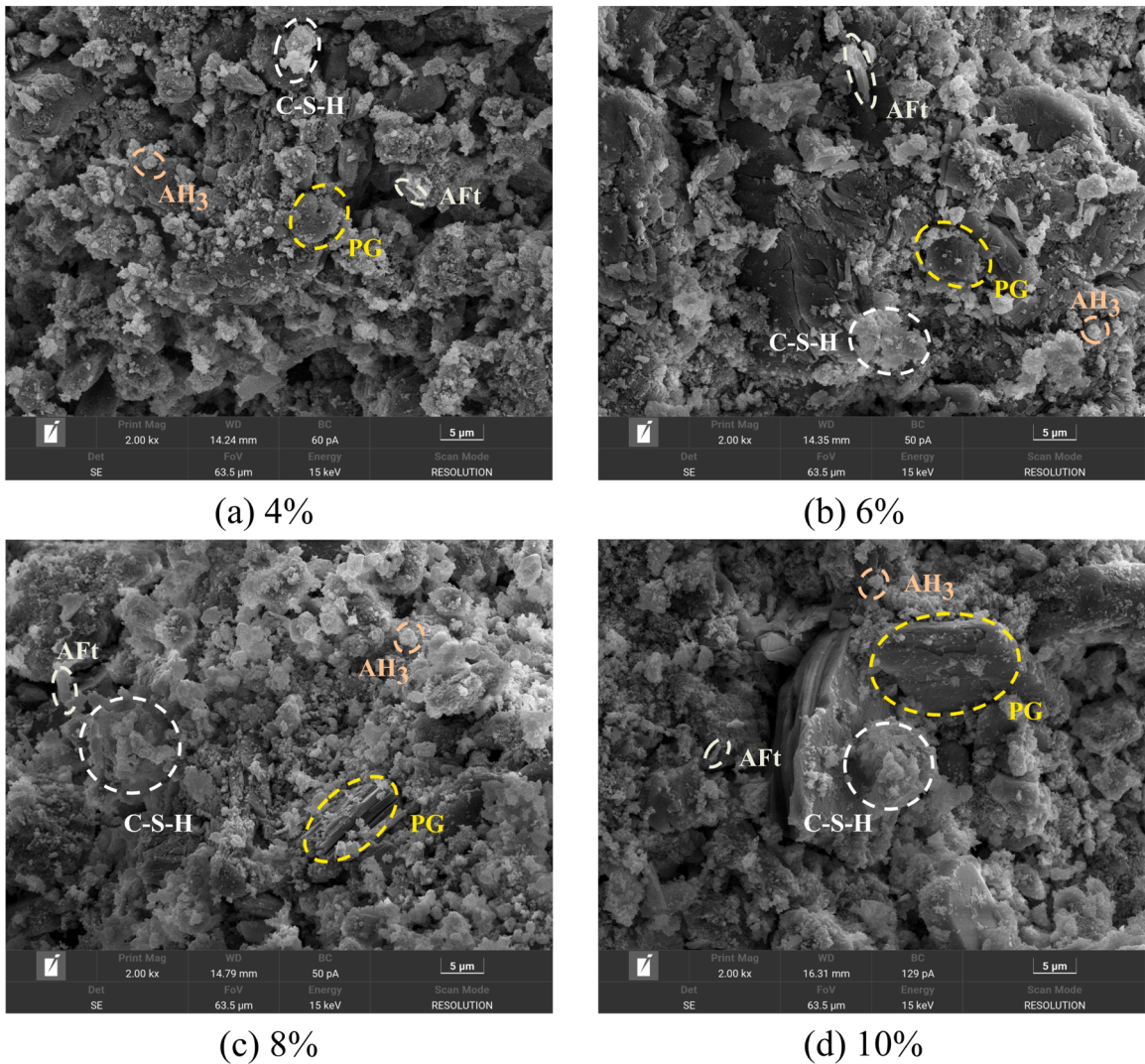
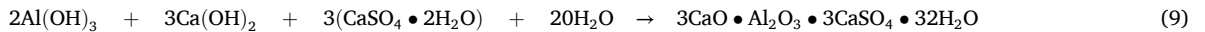


Fig. 9. SEM images of different SAC contents.



### 3.6. Effect of W/S

Microstructure diagrams of different W/S dosages are shown in Fig. 11. It can be seen that with the increase of water incorporation, the hydration products generated per unit area are significantly reduced, and the penetrating pores and cracks are gradually increased. In conjunction with the trend observed in Fig. 10 for compressive strength and thermal conductivity, an increase in W/S from 0.275 to 0.325 leads to a gradual decrease in the compressive strength value of PBCM from 6.40 MPa to 6.34 MPa, exhibiting linearity. However, when W/S increases from 0.325 to 0.35, there is a significant decline in compressive strength accompanied by an initial increase followed by a subsequent decrease in thermal conductivity values. Notably, at W/S = 0.275, PBCM exhibits its highest compressive strength of 6.40 MPa and lowest thermal conductivity value of 0.1961 W/(m·K).

The reason is when W/S is 0.275, the PG without hydration reaction in PBCM will accumulate into a block and aggregate into a dense mass, and the thermal insulation and compressive properties are excellent. As the weight of W/S increases, more PG dissolves in the water, resulting in large porosity and cracks within the test blocks. During heat transfer processes, convective heat exchange occurs. At this instance, the thermal conductivity values increased while the compressive strength values decreased. As water content increases within the range of 0.325–0.35, the alkalinity of the slurry is diluted, leading to a decrease in the rate of hydration reactions and reduced formation of C-S-H gels and AH<sub>3</sub> gels. Unreacted water molecules will gradually be expelled during subsequent maintenance processes, leaving behind a multitude of capillary pores within the material, causing it to become more porous. When subjected to stress, it is more susceptible to stress concentration phenomena, which result in macroscopic cracks that ultimately cause the

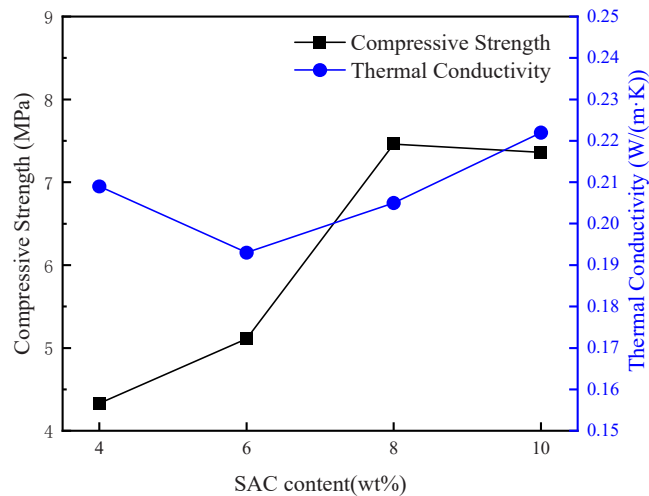


Fig. 8. Effect of SAC content.

sample to damage. At this time, the compressive strength and thermal conductivity values have both decreased [39].

### 3.7. Effect of foam content on cementitious materials

Microstructure diagrams of different foam dosages are shown in Fig. 13. It can be seen that as the foam content increases from 0 % to 8 %, the closed pores in the FPBCM gradually increase, and when the foam content increases from 10 % to 14 %, the closed pores gradually connect into a large number of penetrating pores. Combined with the trends of compressive strength and thermal conductivity of different density grades in Fig. 12 (a), it can be seen from Fig. 12 (a) that the density and compressive strength values of FPBCM decrease with the increase of foam content. Compared to the unmixed foam, the dry density and compressive strength of FPBCM decreased from 1584 kg/m<sup>3</sup> and 11.44 MPa to 1122 kg/m<sup>3</sup> and 3.97 MPa, with a decrease of 29.17 % and 65.30 % when 4 % foam was added. When the foam content was 6 %, the dry density and compressive strength of FPBCM were 1013 kg/m<sup>3</sup> and 3 MPa, respectively, which decreased by 36.05 % and 73.78 % compared to the blank control group. When the foam content is 10 %, the dry density and compressive strength of FPBCM are 683 kg/m<sup>3</sup> and 0.75 MPa, respectively, which is 56.88 % and 93.44 % lower than those of the blank control group, respectively.

As can be seen from Fig. 12 (b), the density and thermal conductivity of FPBCM decrease with the increase of foam content. Compared to the unmixed foam, the thermal conductivity of the cementitious material decreased from 0.2037 W/(m · K) to 0.1454 W/(m · K) when 4 % foam was added, with a decrease of 28.62 %. When the foam content was 6 %, the thermal conductivity of FPBCM was 0.1436 W/(m · K), which decreased by 29.50 % compared to the blank control group. When the foam content was 10 %, the thermal conductivity of FPBCM was 0.1205 W/(m · K), which decreased by 40.84 % compared to the blank control group. However, considering the mechanical properties, the FPBCM with 8 % foam content is the best. The density, compressive strength and thermal conductivity of FPBCM tend to decrease gradually when the foam content is 4~8 %, and tend to be flat when the foam content is 10 %. The reason is when the foam content is less than 4 %, with the increase of foam content, the foam is stable in the process of mixing with the slurry, and the coarsening rupture after the FPBCM is condensed, leaving many fine pores, and the number of pores in the FPBCM increases significantly, which hinders the transfer of heat in the material, and the thermal insulation performance is enhanced, resulting in a significant decrease in the density, compressive strength and thermal conductivity of the test block. However, with the increase of the foam content from 4 % to 8 %, the number of closed pores in the FPBCM increases slowly, and the tiny bubbles reach saturation when the foam content is 8 %, so the density, compressive strength and thermal conductivity of the foam cementitious material decrease slowly in this dosage range. When the foam content increases to 10 %, the internal microfoam of FPBCM begins to connect gradually after saturation, forming a penetrating macropores, which will cause stress concentration in the sample under the action of pressure, resulting in a significant decrease in compressive strength. Due to the increase of macropores and micropores, the density and thermal conductivity of FPBCM also decreased significantly.

## 4. Discussion

### 4.1. Mechanism of hydration

The mechanistic diagram of the CaO-SiO<sub>2</sub>-Al<sub>2</sub>O<sub>3</sub> ternary oxidation system in the composite cementitious material is illustrated in Fig. 14 (a). The contents of CaO, SiO<sub>2</sub>, and Al<sub>2</sub>O<sub>3</sub> are derived from the QL, CCG, SAC, respectively. As shown in Fig. 14 (b), after mixing the slurry, the reaction consumes some of the PG and produces C-S-H gel and Aft. At this time, the CCG in the slurry will disperse SiO<sub>2</sub> and Ca(OH)<sub>2</sub> to interact with each other to generate C-S-H gel, leading to a decrease in the concentration of Ca(OH)<sub>2</sub> and thus

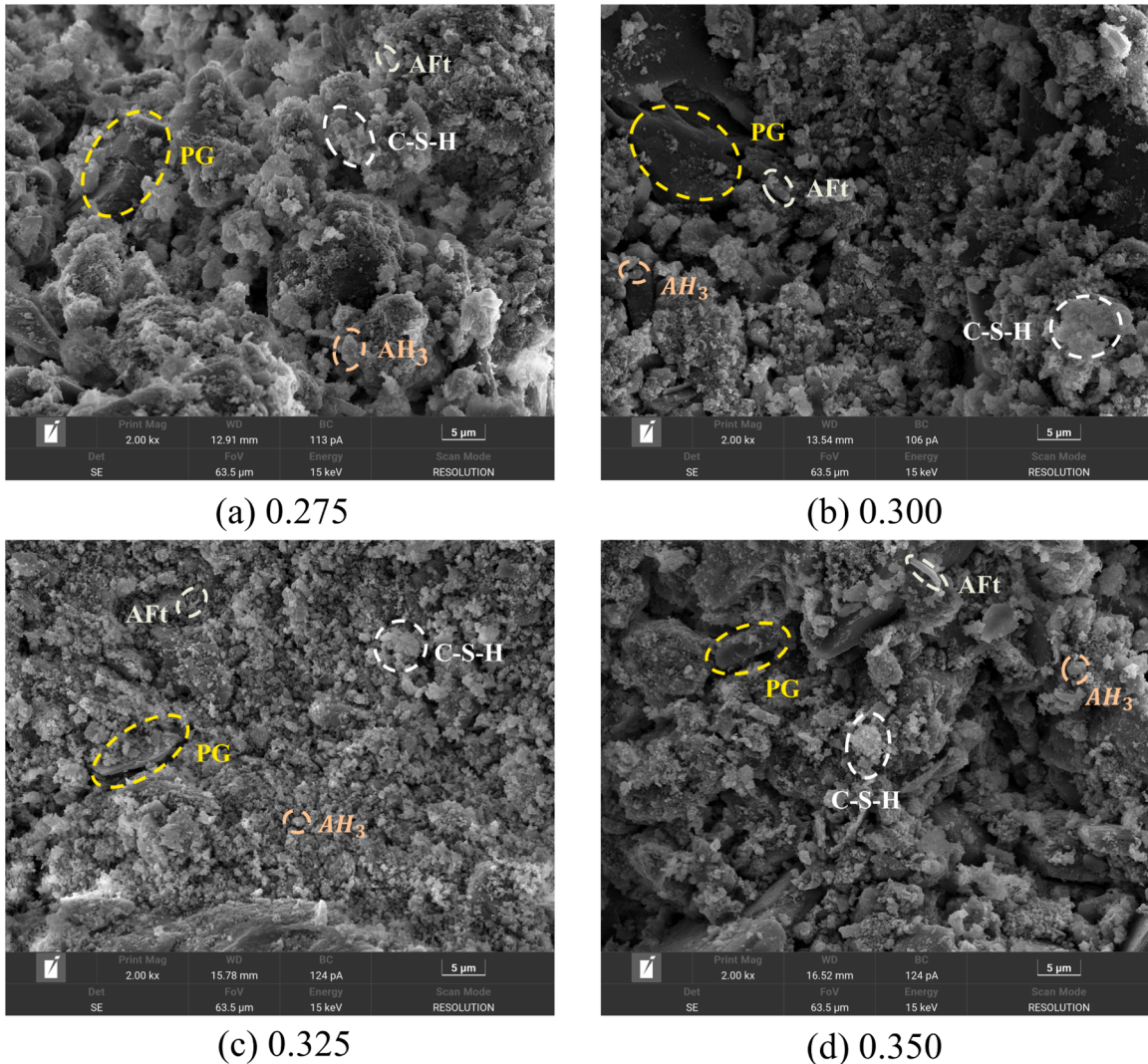


Fig. 11. SEM images with different W/S.

inhibiting the reaction of  $\text{Ca}(\text{OH})_2 \cdot 2\text{H}_2\text{O}$  to generate AFt. That is, the  $\text{CaO-SiO}_2\text{-Al}_2\text{O}_3$  ternary oxidation system was re-adjusted to regulate the ratio of the generation of AFt and C-S-H gel (C-S-H gel increased and AFt decreased). This mechanism effectively explains the gelling properties possessed by CCG as well as the regulatory properties that improve the strength development of composite gelling materials.

#### 4.2. Product performance

The product performance is compared with the foam concrete specification (JG/T266–2011) [40], and the product performance and test results are shown in Table 6. As can be seen from the table, the foam content of 0 %, 2 % and 8 % FPBCM meets the requirements of the specification. The ratio of the best thermal insulation performance of FPBCM was 45 % PG, CCG: cement = 3:7, 8 % QL, 8 % SAC, W/S = 0.275, 8 % foam and 1 % superplasticizer.

The compressive strength value of the FPBCM that meets the compressive requirements and has the best insulation performance in this study is 2.53 MPa, and the thermal conductivity value is 0.1427 W/(m·K). Table 7 presents a performance comparison between this study and others. Zhang et al. [41] prepared foam phosphogypsum-based composite materials by adding various fibers. The performance of the best test pieces was characterized by their compressive strength value of 4.56 MPa and thermal conductivity value of 0.2630 W/(m·K). Compared to FPBCM, the compressive strength has increased by 80.23 %, but the thermal insulation performance has decreased by 84.30 %, resulting in an overall decrease of 4.07 %. Ren et al. [42] prepared cement-based exterior wall insulation materials using polystyrene and cement with different calcium silicate contents. Among them, the best performing test block had a compressive strength value of 0.24 MPa and a thermal conductivity value of 0.0423 W/(m·K). Compared with FPBCM, the

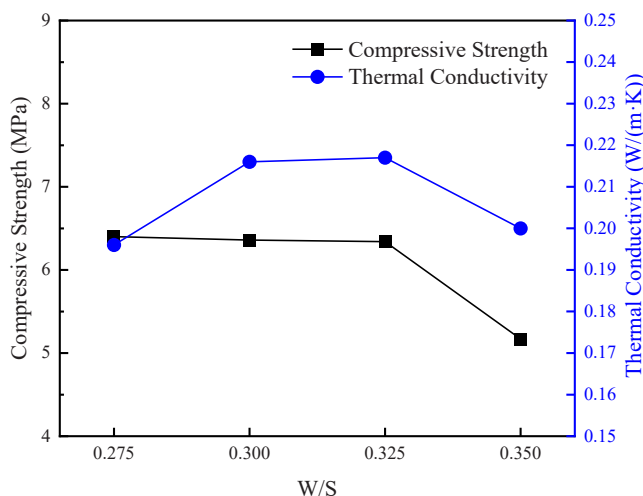


Fig. 10. Effect of W/S.

compressive performance decreased by 90.51 %, the thermal insulation performance improved by 70.36 %, and the overall performance decreased by 20.15 %. Umponpanara et al. [43] employed aluminum sulfate and sodium bicarbonate as gas-producing additives and hemihydrated gypsum as the raw material to prepare foam gypsum. Among them, the most superior test block exhibited a compressive strength value of 2.65 MPa and a thermal conductivity value of 0.2790 W/(m·K). Compared with FPBCM, the compressive performance increased by 4.74 %, but the insulation performance dropped by 95.51 %, resulting in an overall decrease of 90.77 %. Compared with other cement-based materials, the FPBCM developed in this study exhibited certain improvements in overall performance. Furthermore, the lower thermal conductivity of FPBCM renders it particularly suitable for insulation applications. In actual engineering practice, the use of this construction material aids in reducing energy consumption during the building's operational phase, thereby enhancing comfort levels within the indoors.

#### 4.3. Solid waste utilization

The processing and utilization of solid wastes, such as PG and CG, are of great significance in China. Mechanical studies and ratio design were carried out based on the material properties of in-situ PG and CCG to obtain the optimal ratio between the materials. In the case of PG, it is of significant research value to use original PG to study insulation materials with excellent thermal insulation properties in order to maximize the usefulness of PG and reduce energy consumption. The addition of CCG improves the material properties while increasing the solid waste utilization of the gelling material, resulting in a solid waste utilization rate of 56.7 %.

## 5. Conclusions

This study incorporates CCG into FPBCM, aims to enhance the performance of FPBCM and increase the utilization rate of solid waste by adjusting the hydration products, while reducing environmental pollution. Based on the experimental results of this study, the following conclusions can be drawn:

- (1) In PBCM, QL primarily provides the alkaline environment required for hydration of cementitious materials, while untreated PG mainly serves as a filler, with only a small amount participating in the hydration reaction under such conditions. CCG regulates the ratio of AFt to C-S-H gel by means of  $\text{SiO}_2$ , while SAC affects compressive strength and thermal conductivity by accelerating the hydration reaction rate.
- (2) From orthogonal experimentally range analysis, it can be found that the extent to which each factor affected the compressive strength and thermal conductivity of PBCM are as follows: SAC content > PG content > CCG substitution ratio > W/S > QL content.
- (3) Based on the comprehensive evaluation of the compression strength and thermal conductivity of FPBCM, the optimal ratio is 45 % PG, 3/7 for CCG/cement, 8 % for QL, SAC and foam content, 0.275 for W/S, and 1 % for WR.
- (4) The compressive strength value of the composite cementitious material with 8 % foam content is 2.53 MPa, and the thermal conductivity value is 0.1427 W/(m·K). Compared with the test block without foam, the thermal conductivity value decreases by 29.95 %, which enhances the thermal insulation performance.

#### CRedit authorship contribution statement

**Hongwei Wu:** Investigation, Data curation. **Xing Liang:** Validation, Supervision. **Jiri Zhou:** Investigation, Formal analysis. **Zujing**



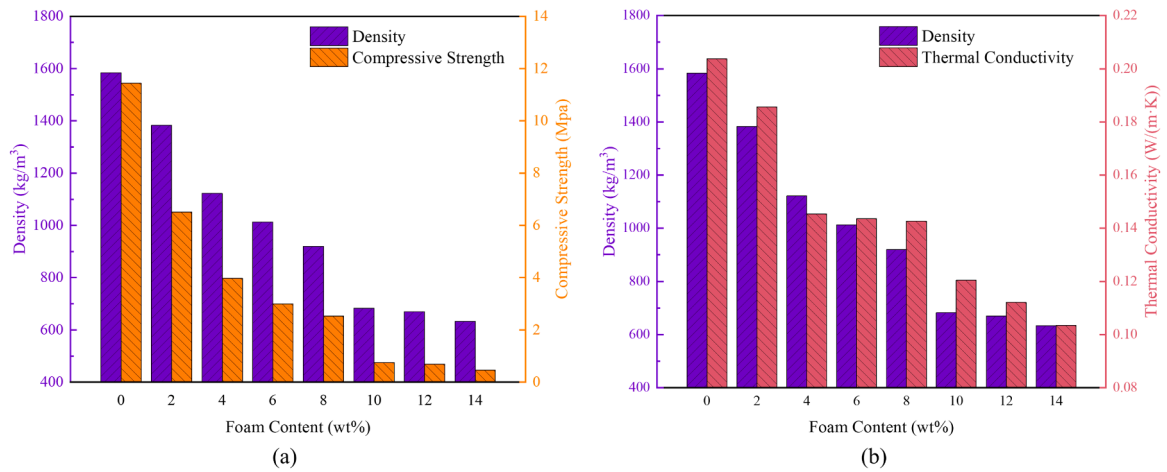


Fig. 12. Effect of foam content: (a) Effect of foam content on density and compressive strength; (b) Effect of foam content on density and thermal conductivity.

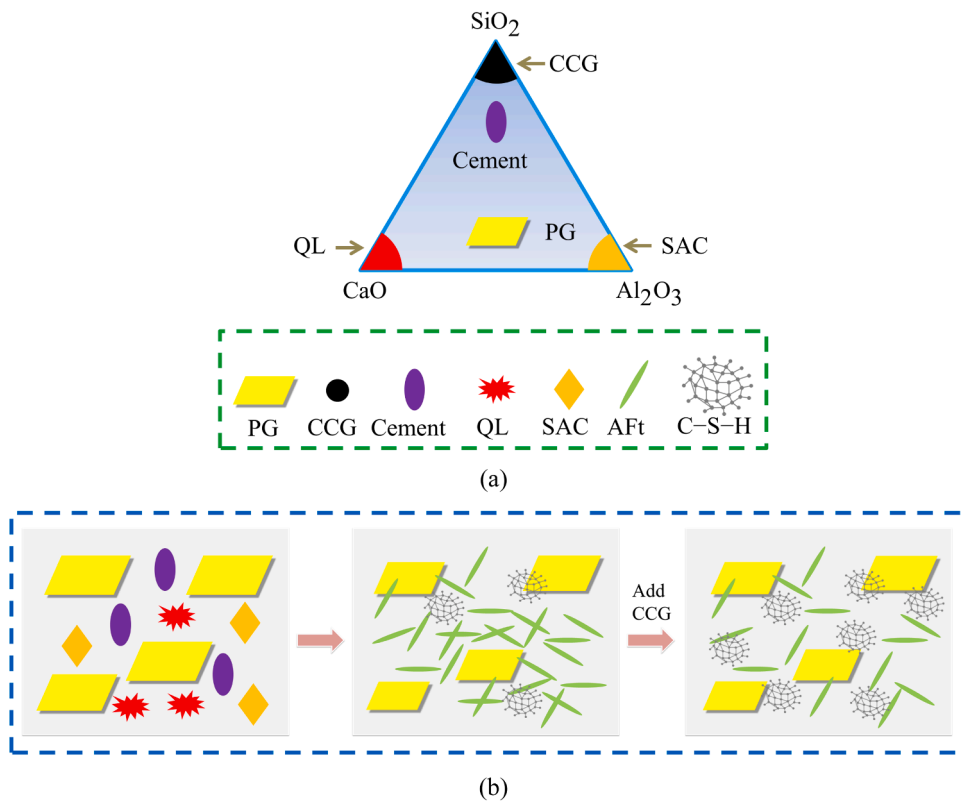


Fig. 14. Hydration mechanism diagram: (a) Ternary oxygen system in composite cementitious materials; (b) Diagram of the hydration mechanism after the addition of CCG.

**Zhang:** Writing – review & editing, Software, Resources, Investigation, Funding acquisition, Formal analysis. **Haoyun Ren:** Writing – review & editing, Writing – original draft, Investigation, Funding acquisition, Formal analysis, Conceptualization. **Ruiyong Mao:** Writing – review & editing, Investigation, Formal analysis.

**Declaration of Competing Interest**

We declare that we have no financial and personal relationships with other people or organizations that can inappropriately

**Table 6**  
Product performance and specification qualification judgment.

Foam dosage	Dry density grade	Test result			Standard			Qualified determination
		Density(kg/m <sup>3</sup> )	Compressive strength (MPa)	Thermal conductivity (W/(m·K))	Dry density $\rho_d$ (kg/m <sup>3</sup> )	Compressive strength (MPa)	Thermal conductivity (W/(m·K))	
0	A16	1584	11.44	0.2037	1550 < $\rho_d$ ≤ 1650	8.0 ~ 30.0	—	Qualified
2	A14	1383	6.51	0.1857	1350 < $\rho_d$ ≤ 1450	5.5 ~ 10.0	—	Qualified
4	A11	1122	3.97	0.1454	1050 < $\rho_d$ ≤ 1150	4.0 ~ 5.5	—	Not qualified
6	A10	1013	3.00	0.1436	950 < $\rho_d$ ≤ 1050	3.5 ~ 5.0	≤ 0.27	Not qualified
8	A09	920	2.53	0.1427	850 < $\rho_d$ ≤ 950	2.5 ~ 4.0	≤ 0.24	Qualified
10	A07	683	0.75	0.1205	650 < $\rho_d$ ≤ 650	1.2 ~ 2.0	≤ 0.18	Not qualified
12	A07	670	0.69	0.1121				Not qualified
14	A06	633	0.46	0.1035	550 < $\rho_d$ ≤ 650	1.0 ~ 1.5	≤ 0.14	Not qualified

**Table 7**  
Product performance comparison.

Research source	Compressive strength (MPa)	Changes in compressive performance	Thermal conductivity (W/(m·K))	Changes in thermal insulation performance	Performance comparison
FPBCM	2.53	—	0.1427	—	100 %
Fiber-reinforced lightweight foamed phosphogypsum-based composite [41]	4.56	+80.23 %	0.2630	−84.30 %	95.93 %
Cement-based external wall insulation material [42]	0.24	−90.51 %	0.0423	+70.36 %	79.85 %
Foamed gypsum [43]	2.65	+4.74 %	0.2790	−95.51 %	9.23 %

influence our work, there is no professional or other personal interest of any nature or kind in any product, service and/or company that could be construed as influencing the position presented in, or the review of, the manuscript entitled '*Preparation and properties of phosphogypsum-based calcined coal gangue composite cementitious materials*'.

## Acknowledgments

The authors would like to thank the financial support from the National Natural Science Foundation of China (NO. 52168013 and NO. 51908080), the Natural Science Foundation of Guizhou Province (No. ZK [2022]151 and No. [2020]2004) and the State Key Laboratory of Gas Disaster Detecting, Preventing and Emergency Controlling Open fund Project (No.2021SKLKF10).

## Data availability

The authors do not have permission to share data.

## References

- [1] L. Bing, S. Jiancheng, C. Mengjun, Z. Xiangfei, L. Renlong, Y. Yong, A new basic burning raw material for simultaneous stabilization/solidification of PO4<sup>3-</sup> and F<sup>-</sup> in phosphogypsum, *Ecotoxicol. Environ. Saf.* 252 (2023) 114582, <https://doi.org/10.1016/j.ecoenv.2023.114582>.
- [2] T.P. Mashifana, Chemical treatment of phosphogypsum and its potential application for building and construction, *Powder Technol.* 35 (2019) 641–648, <https://doi.org/10.1016/j.promfg.2019.06.007>.
- [3] F. Wu, Y. Ren, G. Qu, S. Liu, B. Chen, X. Liu, C. Zhao, J. Li, Utilization path of bulk industrial solid waste: a review on the multi-directional resource utilization path of phosphogypsum, *J. Environ. Manag.* 313 (2022) 114957, <https://doi.org/10.1016/j.jenvman.2022.114957>.
- [4] S. Chen, J. Chen, X. He, Y. Su, Z. Jin, J. Fan, H. Qi, B. Wang, Comparative analysis of colloidal-mechanical microenvironments on the efficient purification of phosphogypsum, *Constr. Build. Mater.* 392 (2023) 132037, <https://doi.org/10.1016/j.conbuildmat.2023.132037>.
- [5] C.-q. Wang, Y. Ying, T. Wang, D.-m. Huang, S. Wei, Highly efficient modified phosphogypsum building gypsum powder and environmentally friendly utilisation in self-levelling mortar, *Arch. Civ. Mech. Eng.* 24 (2) (2024) 118, <https://doi.org/10.1007/s43452-024-00933-6>.
- [6] R.R. Diwa, E.U. Tabora, N.H. Haneklaus, J.D. Ramirez, Rare earths leaching from philippine phosphogypsum using Taguchi method, regression, and artificial neural network analysis, *J. Mater. Cycles Waste Manag.* 25 (6) (2023) 3316–3330, <https://doi.org/10.1007/s10163-023-01753-1>.
- [7] J. Xu, P. Chen, C. Zhang, Y. Yang, Influence of phosphogypsum on mechanical properties and microstructure of iron tailings cementitious material, *Arch. Civ. Mech. Eng.* 24 (1) (2023) 18, <https://doi.org/10.1007/s43452-023-00831-3>.
- [8] N. Mechi, R. Khiari, M. Ammar, E. Elaloui, M.N. Belgacem, Preparation and application of Tunisian phosphogypsum as fillers in papermaking made from *Prunus amygdalus* and *Tamarisk* sp, *Powder Technol.* 312 (2017) 287–293, <https://doi.org/10.1016/j.powtec.2017.02.055>.
- [9] M. Meng, W. Luo, S. Wang, G. Zeng, Predicting the leachate generation from wet phosphogypsum stack using a water-balance-analysis based model, *Environ. Res.* 212 (2022) 113338, <https://doi.org/10.1016/j.envres.2022.113338>.
- [10] S. Zhou, X. Li, Y. Zhou, C. Min, Y. Shi, Effect of phosphorus on the properties of phosphogypsum-based cemented backfill, *J. Hazard. Mater.* 399 (2020) 122993, <https://doi.org/10.1016/j.jhazmat.2020.122993>.
- [11] C. Luo, S. Li, P. Ren, F. Yan, L. Wang, B. Guo, Y. Zhao, Y. Yang, J. Sun, P. Gao, P. Ji, Enhancing the carbon content of coal gangue for composting through sludge amendment: a feasibility study, *Environ. Pollut.* (2024) 123439, <https://doi.org/10.1016/j.envpol.2024.123439>.
- [12] X. Wang, J. Wu, Q. Ma, R. Guo, Y. Zhang, C. Li, Z. Sun, Iron conversion and ammonium salt calcination whitening process and mechanism of pre-calcined coal gangue, *Chem. Eng. Sci.* 287 (2024) 119802, <https://doi.org/10.1016/j.ces.2024.119802>.
- [13] C. Wang, K. Feng, L. Wang, Q. Yu, F. Du, X. Guo, Characterization of coal gangue and coal gangue-based sodalite and their adsorption properties for Cd<sup>2+</sup> ion and methylene blue from aqueous solution, *J. Mater. Cycles Waste Manag.* 25 (3) (2023) 1622–1634, <https://doi.org/10.1007/s10163-023-01630-x>.
- [14] D.-y. Duan, C.-q. Wang, D.-s. Bai, D.-m. Huang, Representative coal gangue in China: physical and chemical properties, heavy metal coupling mechanism and risk assessment, *Sustain. Chem. Pharm.* 37 (2024) 101402, <https://doi.org/10.1016/j.scp.2023.101402>.
- [15] G. Ke, H. Jiang, Z. Li, Study on the calorific value and cementitious properties of coal gangue with 0–1 mm particle size, *Constr. Build. Mater.* 414 (2024) 135061, <https://doi.org/10.1016/j.conbuildmat.2024.135061>.
- [16] X. Li, M. Pan, M. Tao, W. Liu, Z. Gao, C. Ma, Preparation of high closed porosity foamed ceramics from coal gangue waste for thermal insulation applications, *Ceram. Int.* 48 (24) (2022) 37055–37063, <https://doi.org/10.1016/j.ceramint.2022.08.280>.
- [17] B. Peng, D. Guo, H. Qiao, Q. Yang, B. Zhang, T. Hayat, A. Alsaedi, B. Ahmad, Bibliometric and visualized analysis of China's coal research 2000–2015, *J. Clean. Prod.* 197 (2018) 1177–1189, <https://doi.org/10.1016/j.jclepro.2018.06.283>.
- [18] D. Ma, Q. Wang, Z. Tian, B. Zhang, G. Xie, Recovery of sulphur dioxide by converter dust synergistic coke decomposition of phosphogypsum, *Chem. Eng. Sci.* 288 (2024) 119814, <https://doi.org/10.1016/j.ces.2024.119814>.
- [19] R. Pérez-López, F. Macías, C.R. Cánovas, A.M. Sarmiento, S.M. Pérez-Moreno, Pollutant flows from a phosphogypsum disposal area to an estuarine environment: an insight from geochemical signatures, *Sci. Total Environ.* 553 (2016) 42–51, <https://doi.org/10.1016/j.scitotenv.2016.02.070>.
- [20] Q. Zhou, Y. Xu, P. Liu, Y. Qin, H. Zhang, Mechanical properties of energy sustainable round bamboo - phosphogypsum composite floor slabs, *J. Build. Eng.* 76 (2023) 107192, <https://doi.org/10.1016/j.job.2023.107192>.
- [21] K. Gu, B. Chen, Loess stabilization using cement, waste phosphogypsum, fly ash and quicklime for self-compacting rammed earth construction, *Constr. Build. Mater.* 231 (2020) 117195, <https://doi.org/10.1016/j.conbuildmat.2019.117195>.

- [22] Y. Wang, Y. Hu, X. He, Y. Su, B. Strnadell, W. Miao, Hydration and compressive strength of supersulfated cement with low-activity high alumina ferronickel slag, *Cem. Concr. Compos.* 136 (2023) 104892, <https://doi.org/10.1016/j.cemconcomp.2022.104892>.
- [23] C. Ding, T. Sun, Z. Shui, Y. Xie, Z. Ye, Physical properties, strength, and impurities stability of phosphogypsum-based cold-bonded aggregates, *Constr. Build. Mater.* 331 (2022) 127307, <https://doi.org/10.1016/j.conbuildmat.2022.127307>.
- [24] Y. Li, S. Dai, Y. Zhang, J. Huang, Y. Su, B. Ma, Preparation and thermal insulation performance of cast-in-situ phosphogypsum wall, *J. Appl. Biomater. Funct. Mater.* 16 (1\_) (2018) 81–92, <https://doi.org/10.1177/2280800017751487>.
- [25] Y. Zhu, Y. Zhu, A. Wang, D. Sun, K. Liu, P. Liu, Y. Chu, Valorization of calcined coal gangue as coarse aggregate in concrete, *Cem. Concr. Compos.* 121 (2021) 104057, <https://doi.org/10.1016/j.cemconcomp.2021.104057>.
- [26] Y. Liu, S. Lei, M. Lin, Y. Li, Z. Ye, Y. Fan, Assessment of pozzolanic activity of calcined coal-series kaolin, *J. Mater. Cycles Waste Manag.* 143 (2017) 159–167, <https://doi.org/10.1016/j.jclay.2017.03.038>.
- [27] C. Astm, Standard Specification for Coal Ash and Raw or Calcined Natural Pozzolan for Use in Concrete, 618, *ASTM international*, 2023.
- [28] C. Wang, C. Liu, L. Zhang, C. Wang, S. Xu, J. Yang, Exploring calcined coal gangue fines as the total substitute of fly ash in the production of alkali-activated slag/fly ash materials, *Case Stud. Constr. Mater.* 17 (2022) e01332, <https://doi.org/10.1016/j.cscm.2022.e01332>.
- [29] Z. Guo, J. Xu, Z. Xu, J. Gao, X. Zhu, Performance of cement-based materials containing calcined coal gangue with different calcination regimes, *J. Build. Eng.* 56 (2022) 104821, <https://doi.org/10.1016/j.job.2022.104821>.
- [30] B. Yao, G. Ren, J. Huang, X. Gao, Influence of self-ignition coal gangue on properties of foam concrete with steam curing, *Case Stud. Constr. Mater.* 17 (2022) e01316, <https://doi.org/10.1016/j.cscm.2022.e01316>.
- [31] X. Guan, J. Chen, M. Zhu, J. Gao, Performance of microwave-activated coal gangue powder as auxiliary cementitious material, *J. Mater. Res. Technol. JMRT* 14 (2021) 2799–2811, <https://doi.org/10.1016/j.jmrt.2021.08.106>.
- [32] Z. Wang, Z. Shui, T. Sun, T. Hu, X. Xiao, J. Fan, Reutilization of gangue wastes in phosphogypsum-based excess-sulphate cementitious materials: effects of wet co-milling on the rheology, hydration and strength development, *Constr. Build. Mater.* 363 (2023) 129778, <https://doi.org/10.1016/j.conbuildmat.2022.129778>.
- [33] T. Tian, Y. Yan, Z. Hu, Y. Xu, Y. Chen, J. Shi, Utilization of original phosphogypsum for the preparation of foam concrete, *Constr. Build. Mater.* 115 (2016) 143–152, <https://doi.org/10.1016/j.conbuildmat.2016.04.028>.
- [34] S. Wang, Z. Chen, H. Jiang, J. Su, Z. Wu, Strength performance and enhancement mechanism of silty sands stabilized with cement, red mud, and phosphogypsum, *J. Build. Eng.* 73 (2023) 106762, <https://doi.org/10.1016/j.job.2023.106762>.
- [35] GB/T 17669.3-1999[S], (1999). The State Bureau of Quality and Technical Supervision. Gypsum plasters-Determination of Mechanical Properties.
- [36] GB/T 10294-2008[S], (2008). General Administration of Quality Supervision, Inspection and Quarantine of the People's Republic of China, Standardization Administration of the People's Republic of China. Thermal Insulation Determination of Steady-state Thermal Resistance and Related Properties-Guarded Hot Plate Apparatus.
- [37] M. Chen, P. Liu, D. Kong, Y. Wang, J. Wang, Y. Huang, K. Yu, N. Wu, Influencing factors of mechanical and thermal conductivity of foamed phosphogypsum-based composite cementitious materials, *Constr. Build. Mater.* 346 (2022) 128462, <https://doi.org/10.1016/j.conbuildmat.2022.128462>.
- [38] Y. Cheng, L.A.-O.X. Li, P. Zhou, Y. Zhang, H. Liu, Multi-objective optimization design and test of compound diatomite and basalt fiber asphalt mixture, *Materials* (1996-1944) (2019), <https://doi.org/10.3390/ma12091461>.
- [39] Y. Zhao, C.L. Wang, J. Bi, Analysis of fractured rock permeability evolution under unloading conditions by the model of elastoplastic contact between rough surfaces, *Rock. Mech. Eng.* 53 (12) (2020) 5795–5808, <https://doi.org/10.1007/s00603-020-02224-x>.
- [40] JG/T266-2011[S], *Foamed Concrete*, General Administration of Quality Supervision, Inspection and Quarantine of PR China, Beijing, 2011.
- [41] L. Zhang, K.H. Mo, T.H. Tan, S.P. Yap, F.W. Lee, T.-C. Ling, Synthesis and characterization of fiber-reinforced lightweight foamed phosphogypsum-based composite, *Constr. Build. Mater.* 394 (2023) 132244, <https://doi.org/10.1016/j.conbuildmat.2023.132244>.
- [42] W.R. Ren, C.H. Wang, C.B. Han, D. Han, J.Y. Zheng, Y.N. Cui, X.M. Song, Q. Jiang, H. Yan, Cement-based external wall insulation material with thermal performance improvement by partial substitution of calcium silicate, *Energy Build.* 317 (2024) 114415, <https://doi.org/10.1016/j.enbuild.2024.114415>.
- [43] P. Umponpanarat, S. Wansom, Thermal conductivity and strength of foamed gypsum formulated using aluminum sulfate and sodium bicarbonate as gas-producing additives, *Mater. Struct.* 49 (4) (2016) 1115–1126, <https://doi.org/10.1617/s11527-015-0562-1>.